*Soon-Bok Lee**

Out-of-Phase, Combined Bending and Torsion Fatigue of Steels

REFERENCE Soon-Bok, Lee, **Out-of-phase, combined bending and torsion fatigue of steels**, *Biaxial and Multiaxial Fatigue*, EGF 3 (Edited by M. W. Brown and K. J. Miller), 1989, Mechanical Engineering Publications, London, pp. 621–634.

ABSTRACT The relative abilities of two commonly used criteria together with a more recent approach to predict fatigue strength under 90 degree out-of-phase combined bending and torsion are compared, using discriminating specimens. Tests were performed for two pressure vessel steels, namely type 304 stainless and A533B. In the intermediate- to high-cycle regime, the new approach predicted failure adequately for the out-of-phase combined loading, whereas the conventional criteria overestimated fatigue strength.

Results of further exploratory tests with A533B steel and an SM45C structural steel to investigate the influence of (i) normal stress amplitude acting on a plane of maximum amplitude of shear stress, and (ii) mean bending stress, on fatigue life are discussed. Normal stress amplitude significantly reduced fatigue life in A533B, but mean normal stress had little influence for the stress combinations tested. The influence of the mean bending stress, which reduced the fatigue life in 90 degree out-of-phase bending–torsion tests of SM45C steel, was predicted by combining the uniaxial mean stress effect with the new criterion for fully-reversed out-of-phase torsion and bending.

Introduction

Multiaxial fatigue design methods are generally based on the Tresca or von Mises criteria, which assume that the range of either maximum shear stress (or strain) or octahedral shear stress (or strain), respectively, can be used to predict life in complex stress situations from uniaxial fatigue data. Comprehensive reviews **(1)**–**(3)** of multiaxial fatigue show the following trends for smooth specimens made of ductile metals. The Tresca and von Mises criteria appear to correlate reasonably well with fatigue strength under high-cycle, proportional stressing. However, for low-cycle fatigue with proportional straining, the criteria do not perform as well. For instance, they may overestimate fatigue strength when a significant tensile hydrostatic stress is present.

Many structural components and machine parts experience out-of-phase multiaxial loadings, causing non-proportional straining in which principal strain proportions and directions change during cycling. Although test data for those conditions are rather limited, it appears that maximum shear stress and octahedral shear stress criteria may substantially overestimate fatigue strength in both high-cycle **(4)(5)** and low-cycle **(6)** regimes. One plausible explanation for this deficiency is that the criteria do not account for the influence of normal stress or strain acting on planes experiencing shear stress or strain **(6)**–**(10)**.

* Department of Mechanical Engineering for Production, Korea Institute of Technology, Taejeon, Korea.

The first purpose of this paper is to present the results of a comparison of the maximum shear stress and octahedral shear stress criteria and a more recent approach, using 'discriminating' specimens subjected to 90 degree out-of-phase, fully-reversed combined bending and torsion, in the intermediate to high-cycle regime. The concept and use of discriminating specimens in fatigue research was described by Fuchs (**11**). Such specimens permit a simultaneous and relative comparison of the abilities of different fatigue criteria to predict failure under a given type of loading. The location of failure on a specimen indicates which of the criteria is superior.

The second purpose of the paper is to report the results of an exploratory study of the influence on 90 degree out-of-phase fatigue of normal stress amplitude and mean normal stress on a plane of maximum shear stress amplitude. The third purpose is to propose a fatigue life prediction method for out-of-phase torsion and bending with mean bending stress.

Notation

b	Bending fatigue strength
K_t	Elastic stress concentration factor
$SALT$	Equivalent stress according to Langer criterion
$SEQA$	Equivalent stress according to modified Langer criterion
$SGAR$	Equivalent stress according to Garud's empirical criterion
$SLEE$	Equivalent stress according to Lee's empirical criterion
S_a	Alternating stress
S_m	Mean stress
S_u	Ultimate tensile strength
S_f	Fully-reversed stress
$S_f(SALT)$	Equivalent fully-reversed stress by $SALT$ for mean stress effect
$S_f(SEQA)$	Equivalent fully-reversed stress by $SEQA$ for mean stress effect
$S_f(SLEE)$	Equivalent fully-reversed stress by $SLEE$ for mean stress effect
t	Time
T	Torsional fatigue strength
β	Empirical constant for a given metal
σ	Normal stress
σ_a	Amplitude of fully-reversed normal stress due to bending
σ_m	Mean bending stress
τ	Shear stress
τ_a	Amplitude of fully-reversed shear stress due to torsion
K	$2\tau_a/\sigma_a$
ϕ	Phase angle between bending and torsion
n	Empirical mean stress exponent
w	Frequency of sinusoidal loading
θ	Plane angle measured from the transverse plane of a specimen
θ_τ	Planes of maximum amplitude of τ
$\lvert\tau\rvert_{max}$	Amplitude of τ on θ_τ
$\lvert\sigma\rvert_{\theta_\tau}$	Amplitude of σ on θ_τ

Some multiaxial fatigue criteria

Langer criterion

Langer (**12**) proposed an extension of the Tresca criterion for application to non-proportional cyclic stressing, which has been adopted in pressure vessel design (**13**). Briefly, the procedure seeks the largest range of maximum shear stress in a multiaxial stress history and uses one-half of the corresponding (uniaxial) equivalent stress range to compute damage from uniaxial *S–N* data. For synchronous, fully-reversed, out-of-phase bending and torsion ($\sigma = \sigma_a \cos wt$, $\tau = \tau_a \cos(wt + \phi)$), the equivalent stress amplitude ($SALT$) based on that procedure (**14**)(**15**) is

$$SALT = \frac{\sigma_a}{\sqrt{2}} \{1 + K^2 + \sqrt{(1 + 2K^2 \cos 2\phi + K^4)}\}^{1/2} \tag{1}$$

where σ_a = applied bending stress amplitude, τ_a = applied torsional stress amplitude, $K = 2\tau_a/\sigma_a$, and ϕ is the phase angle between bending and torsion. When $\phi = 90$ degrees, equation (1) reduces to

$$SALT = \begin{cases} 2\tau_a & \text{for } K \geq 1 \quad \text{(2a)} \\ \sigma_a & \text{for } K < 1 \quad \text{(2b)} \end{cases}$$

Modified Langer criterion

A modification of Langer's method, adopted in elevated temperature pressure vessel design (**16**), seeks an equivalent strain range similar to an octahedral shear strain range, by a procedure analogous to that used in finding the maximum shear stress amplitude for non-proportional stressing.

Based on that procedure and expressed in terms of an elastically-calculated stress, the equivalent stress amplitude ($SEQA$) for out-of-phase bending and torsion (**14**)(**15**) is

$$SEQA = \frac{\sigma_a}{\sqrt{2}} \{1 + \tfrac{3}{4}K^2 + \sqrt{(1 + \tfrac{3}{2}K^2 \cos 2\phi + \tfrac{9}{16}K^4)}\}^{1/2} \tag{3}$$

When $\phi = 90$ degrees, equation (3) reduces to

$$SEQA = \begin{cases} \sqrt{3}\tau_a & \text{for } K \geq 2/\sqrt{3} \quad \text{(4a)} \\ \sigma_a & \text{for } K < 2/\sqrt{3} \quad \text{(4b)} \end{cases}$$

Lee criterion

An empirical criterion for fully-reversed, high-cycle out-of-phase bending and torsion fatigue, derived as an extension of Gough's ellipse quadrant (**17**)(**18**), has been proposed by Lee (**15**). The equivalent stress is

$$SLEE = \sigma_a \left\{1 + \left(\frac{b}{2T} K\right)^{\alpha}\right\}^{1/\alpha}; \qquad \alpha = 2(1 + \beta \sin \phi) \tag{5}$$

where b and T are the bending and torsional fatigue strengths respectively, at a

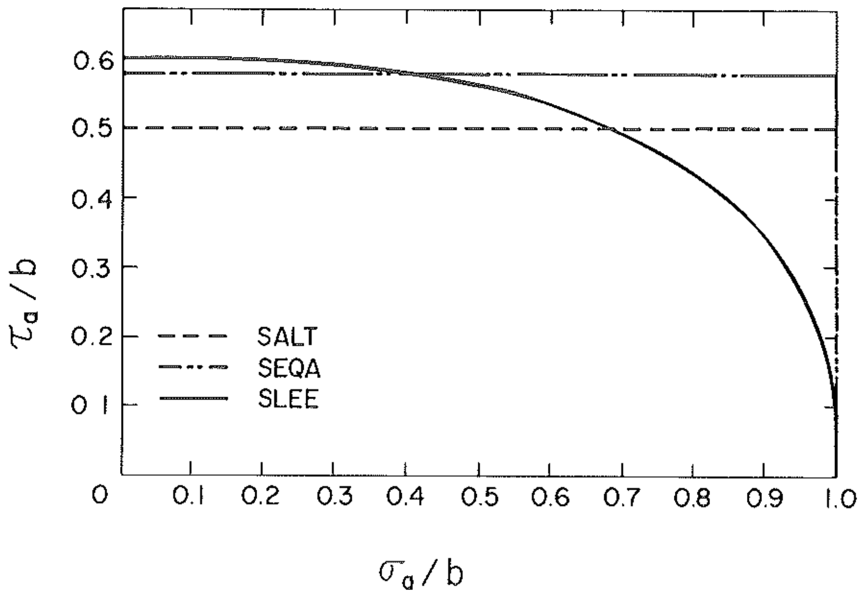

Fig 1 Curves of constant equivalent stress for 90 degree out-of-phase bending and torsion according to three hypotheses. Bending and torsion stresses are normalized by the fatigue strength in bending, b

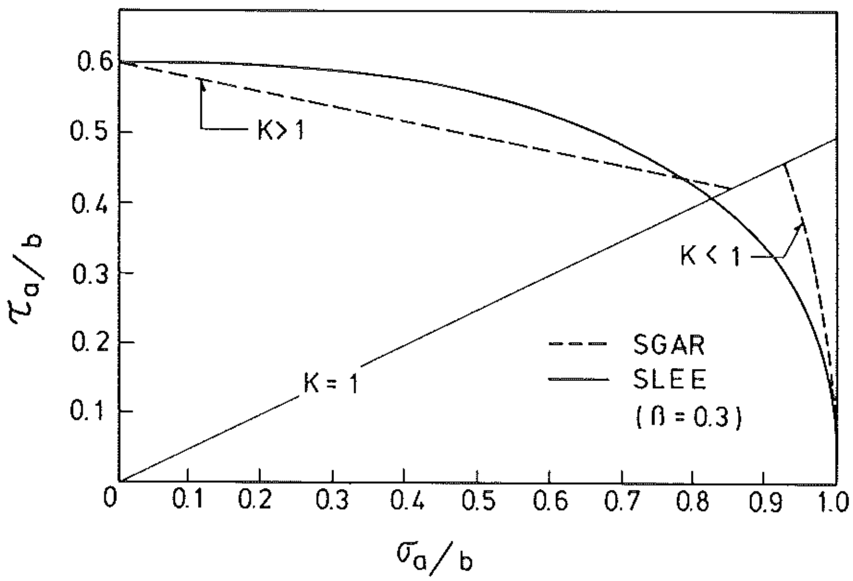

Fig 2 Comparison of *SLEE* and *SGAR* criteria for 90 degree out-of-phase bending and torsion, for $T/b = 0.6$

given life, and β is an empirical constant for a given metal. For a number of ductile metals, T/b is approximately 0.6 and β is about 0.3. Figure 1 compares the above three criteria for various combinations of bending and torsion with $\phi = 90$ degrees. Note that the *SALT* and *SEQA* criteria are insensitive to applied bending stress amplitude when $\phi = 90$ degrees. Also, as shown in Fig. 2, the *SLEE* criterion is relatively close (particularly at $K = 1$) to one initially proposed by Garud and reported in **(11)**.

Garud's criterion for 90 degree out-of-phase bending and torsion was based on the assumption that the maximum amplitude of shear stress and a fraction of the maximum amplitude of normal stress acting on the plane of maximum shear stress amplitude should govern high-cycle fatigue strength. This criterion is similar in spirit to that proposed by Kanazawa *et al.* **(6)** and is given by

$$SGAR = \begin{cases} \sigma_a\left(\dfrac{b}{2T}K + 2 - \dfrac{b}{T}\right) & \text{for } K > 1 \quad \text{(6a)} \\ \sigma_a\left\{\dfrac{b}{2T} + \left(1 - \dfrac{b}{2T}\right)\sqrt{(1 + K^2)}\right\} & \text{for } K < 1 \quad \text{(6b)} \end{cases}$$

where $\phi = 90$ degrees.

Description of materials

Two steels used in nuclear pressure vessels and piping, and one steel used for crankshafts and structural components were tested; namely AISI 304 stainless, A533B, and SM45C. Specimens made from SS304 were annealed at 1050°C for one hour in a hydrogen atmosphere, after final polishing. Specimens of A533B

Table 1 Mechanical properties of the steels tested

	Stainless steel Type 304	*Pressure vessel steel A533B*	*Structural steel SM45C*
Material form	35 mm dia. bar	209 mm thick plate	38 mm dia. bar
Specification	QQ-S-7638 ASTM-A276-67		
Ultimate tensile strength (MPa)	644	576	824
Tensile yield stress (MPa)	289	432	638
Young's modulus* (GPa)	186	213	213
Shear modulus (GPa)	73	83	82.5
Poisson's ratio*	0.28	0.28	0.29
Elongation (%)	64	24	22
Reduction of area (%)	73	63	54
Hardness (Bhn)	163		274

Sources: (1) Data from vendor's records for stainless steel type 304.
(2) Nuclear pressure vessel steel data base report, EPRI-NP-933 (1978), for A533B.
(3) Tensile test results for SM45C structural steel.
* Measured according to ASTM Standard E111 and E132.

Table 2 Chemical composition of the steels tested

	C	*Mn*	*P*	*S*	*Si*	*Ni*	*Cr*	*Mo*	*V*	*Cu*
SS304	0.07	0.92	0.03	0.02	0.85	8.03	20.91	–	–	–
A533B	0.25	1.85	0.03	0.01	0.45	0.73	0.07	0.53	0.21	0.16
SM45C	0.42	0.73	0.02	0.012	0.28	0.14	0.18	–	–	0.13

Compositions were obtained by crystal dispersive spectrometer (SS304, A533B) and emission spectrometer (SM45C).

were taken from the rolling direction of a plate which had been stress-relieved at 620°C for 50 hours. Specimens made from SM45C structural steel were heat-treated at 850°C for 10 minutes and tempered at 650°C for 30 minutes after water-quenching from 850°C. The mechanical properties and chemical composition of these steels are given in Tables 1 and 2, respectively.

Discriminating test specimens

A circular cross-section beam specimen was loaded in deflection-controlled cantilever bending and torsion. By varying the cross-section along the length of the specimen, it was possible to design it with three test sections A, B, and C, as shown in Fig. 3(a). The moving end of each specimen had a steel ball attached to facilitate bending deflection measurements.

The bending and torsional stresses along the longitudinal surface of the specimen, as shown in the thick line curve of Fig. 4, were computed elastically from applied deflections and rotations using a numerical integration of Castigliano's theorem and taking into account the mild stress concentrations at each test section. (K_t values for bending and torsion were less than 1.04 at all sections). The maximum torsional stress occurs at test section A near the moving end and the maximum bending stress occurs at test section C near the fixed end of the specimen. The nominal torsional stress amplitude is one half of the nominal bending stress amplitude at test section B. The equivalent stresses according to the *SALT*, *SLEE*, and *SEQA* criteria, normalized by their respective maximum values, are shown in Table 3 and Fig. 3(b). The highest values of each type of equivalent stress occur at test sections A, B, and C,

Table 3 Stress conditions for the discriminating specimen, taking $\beta = 0.3$ and $T/b = 0.6$

		Normalized equivalent stress (%)		
Test section	$K = 2\tau_a/\sigma_a$	*SALT*	*SLEE*	*SEQA*
A	2.10	100	86	92
B	1.0	88	100	93
C	0.53	95	94	100

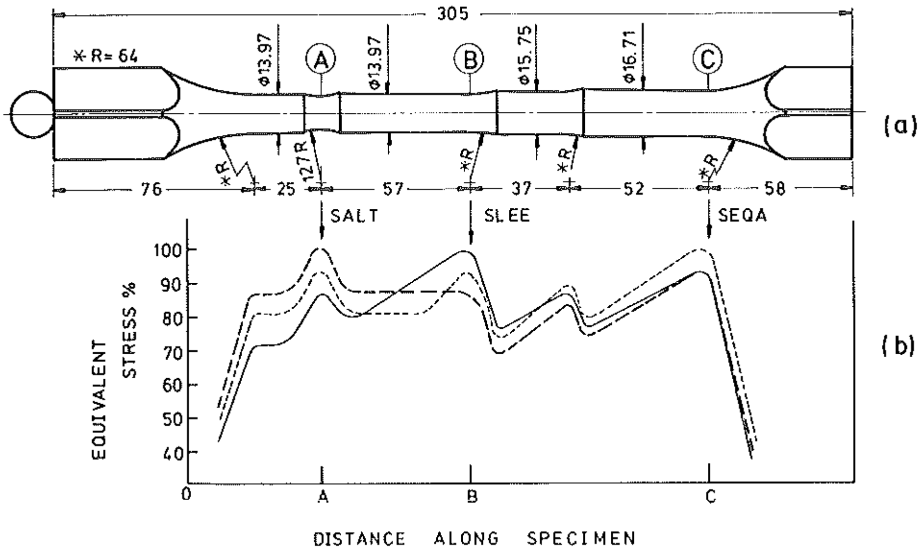

Fig 3 A specimen for discrimination of fatigue criteria under combined bending and torsion, (a) specimen geometry (dimensions in mm), A, B, and C indicate the test sections, and (b) normalized equivalent stresses along the specimen according to the *SALT*, *SLEE*, and *SEQA* criteria

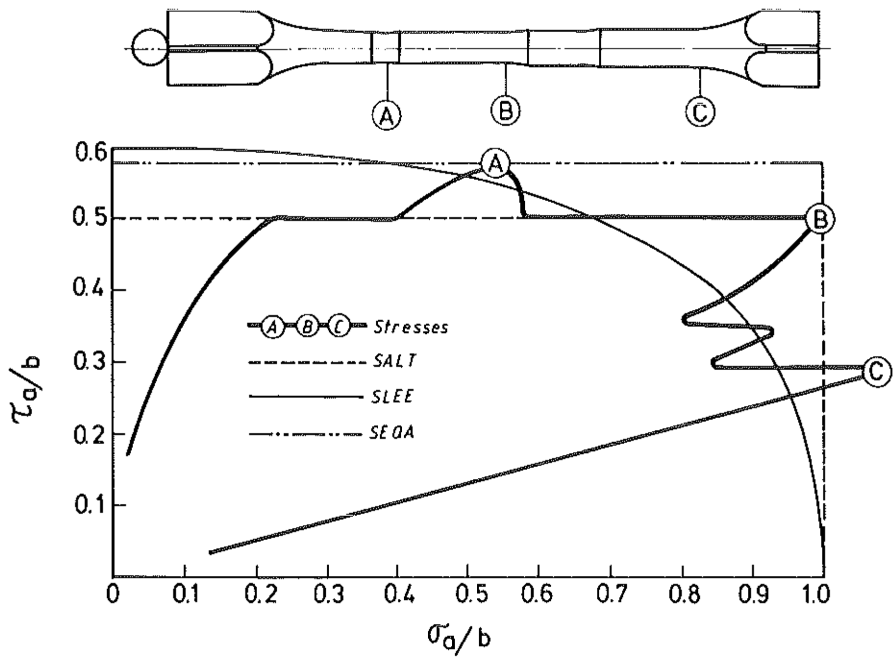

Fig 4 Bending and torsional stresses along the longitudinal surface of the discriminating specimen. Stresses are normalized by the nominal bending stress at the test section B

respectively. Specimens should fail at section A if the Langer criterion is better able to predict fatigue life and at C if the modified Langer criterion is superior. Specimens should fail at B if the *SLEE* criterion is a better predictor for 90 degree out-of-phase bending and torsion.

Discriminating specimen test results

Results of the 90 degree out-of-phase tests are given in Table 4. Here SS denotes specimens made of 304 stainless steel and AS specimens made of A533B. At test section B, the applied torsional stress is nominally one-half of the listed bending stress value. All tests were conducted at room temperature, in laboratory air, and at a frequency of 200 cycles/min. For the tests of AS03, AS07, and AS08, applied deflections were increased in steps to produce failure. Failure was taken as a 10 per cent drop in the specimen bending stiffness. This drop corresponded to an easily visible surface crack of 5–10 mm in length.

All 18 specimens developed cracks at test section B, which experienced lower Langer and modified Langer equivalent stresses than at the other sections. One specimen (SS08) also developed a crack at section A, under a high test loading. Most of the cracks at section B intersected the surface plane with an angle θ

Table 4 Results of discriminating specimen tests

	Applied deflections			*Life (kilocycles)*		
Specimen	*Bending (mm)*	*Torsion (degrees)*	*Elastically calculated bending stress at B (MPa)*	*Step length*	*Total life*	*Crack location*
SS04	3.30	2.15	248		220	B
SS05	3.30	2.15	248		230	B
SS06	3.30	2.15	248		222	B
SS07	4.58	2.99	345		56	B
SS08	4.58	2.99	345		61	A, B
SS09	4.58	2.99	345		51	B
SS10	3.15	2.08	237		368	B
SS11	2.90	1.92	218		427	B
SS12	2.62	1.73	201		913	B
AS01	3.37	2.23	290		478	B
AS02	3.37	2.23	290		459	B
AS03	3.30	2.22	284	507		
	3.37	2.23	290	77	584	B
AS04	3.72	2.49	320		312	B
AS05	3.77	2.49	324		254	B
AS06	3.76	2.49	323		256	B
AS07	2.92	1.93	251	4000		
	3.21	2.11	275	367	4363	B
AS08*	2.91	1.92	251	4000		
	3.22	2.11	275	393	4393	B
AS09	4.88	3.23	420		52	B

* In-phase bending and torsion are applied for AS08.

Table 5 Combinations of shear and normal stress amplitudes for specimen SS12, bending stress amplitude 201 MPa at B

Test section	*K*	θ_τ (*deg.*)	$\lvert\tau\rvert_{max}$ (*MPa*)	$\lvert\sigma\rvert_{\theta_\tau}$ (*MPa*)
A	2.10	0/90	114	109/0
		0		201
B	1.00	45/135	101	142
		90		0
C	0.53	45/135	109	123

between 0 and 10 degrees, where θ is the angle measured on the surface from the transverse plane of a specimen. A few cracks occurred on planes with θ between 10 and 20 degrees.

The results of these tests strongly indicate that the Langer and modified Langer criteria are not adequate predictors for out-of-phase bending and torsion.

The shear and normal stresses at time t on a plane perpendicular to the specimen surface, inclined at an angle θ as defined previously, are

$$\tau(\theta, t) = \tau_a\{\cos(wt + \phi)\cos 2\theta + (1/K)\cos wt \sin 2\theta\} \tag{7}$$

$$\sigma(\theta, t) = \frac{\sigma_a}{2}\{\cos wt(1 + \cos 2\theta) - K\cos(wt + \phi)\sin 2\theta\} \tag{8}$$

When maximized with respect to θ and t for $\phi = 90$ degrees, equation (7) gives the planes of maximum amplitude of shear stress, θ_τ, and the values of those amplitudes, $\lvert\tau\rvert_{max}$. Corresponding normal stress amplitudes on those planes, $\lvert\sigma\rvert_{\theta_\tau}$ are then computed from equation (8). Values of θ_τ, $\lvert\tau\rvert_{max}$ and $\lvert\sigma\rvert_{\theta_\tau}$ are given in Table 5 for test sections A, B, and C of a typical specimen. The other specimens had similar stress distributions, scaled by the applied loading.

With $\phi = 90$ degrees and $K = 1$, all planes normal to the surface at test section B experienced the same maximum amplitude of shear stress, but different values of normal stress amplitude. It is significant that failures occurred at B, which has a lower shear stress amplitude than at A, but a higher normal stress amplitude.

The previous observation that most cracks at B occurred on planes between 0 and 10 degrees, with a few between 10 and 20 degrees, is reasonable when the variation of normal stress amplitude with θ is considered. At 10 degrees, the amplitude drops by only about 3 per cent from its maximum value at $\theta = 0$ degrees. At 20 degrees the drop is approximately 10 per cent.

Tests for normal stress influence

Test results from the discriminating specimens showed that the amplitude of the maximum shear stress or of the octahedral shear stress is not sufficiently accurate to predict fatigue strength under the out-of-phase conditions investigated. The results also provided indirect evidence that at section B, the normal stress amplitude acting on planes of maximum shear stress amplitude probably had an important, secondary influence on fatigue strength. Exploratory tests were performed to further investigate that influence, as well as that of mean normal stress, on high-cycle, 90 degree out-of-phase bending–torsion fatigue of A533B. Of the two pressure vessel steels available for testing, A533B was selected as being the more likely to exhibit a mean normal stress effect, since SS304 has substantial cyclic plastic straining even at lives of 10^6 cycles.

Test specimen and loading

A deflection-controlled, cantilever bending–torsion specimen was used, as shown in Fig. 5. The test section is the reduced diameter portion of the bar. All tests were conducted with $K > 1$, in which case the surface planes of maximum amplitude of shear stress are at $\theta = 0$ degrees and 90 degrees. For $\theta = 0$ degrees, the applied cyclic and static bending stresses are the alternating normal and mean normal stresses on the plane of maximum shear stress amplitude. At locations T and C of the test section, tensile and compressive mean normal stresses are present. Both T and C have the same amplitudes of normal and shear stress. Stress concentration factors at the test section, in bending and torsion, were less than 1.02, and were taken into account in the stress computation.

The 90 degree out-of-phase combinations of applied torsional and bending stresses were selected to be low enough to minimize plastic straining, which could reduce or eliminate any mean stress effects, and yet high enough so that testing could be completed in a reasonable amount of time, producing lives of the order of 10^6 cycles.

Test results

Table 6 gives the results of the exploratory normal stress effect tests. Failure was again taken as a 10 per cent drop in specimen bending stiffness. Specimens

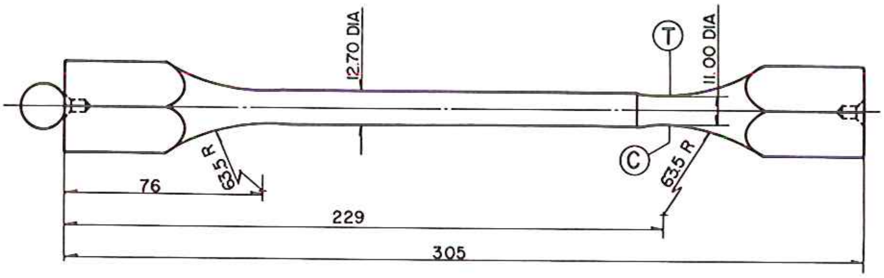

Fig 5 Bending-torsion fatigue specimen for normal stress effect tests. Dimensions in mm

Table 6 Results of normal stress effect tests on A533B pressure vessel steel

Group	*Torsional stress amplitude (MPa)*	*Bending stress amplitude (MPa)*	*Bending mean stress (MPa)*	*Life (kilocycles)*	*Crack location*
Ia	200	200	0	295	top
	200	200	0	362	bottom
	200	200	0	310	bottom
Ib	200	150	0	1106	top
	200	150	0	908	top
	200	150	0	844	bottom
Ic	200	100	0	2500	tests suspended
	200	100	0	2500	
Id	190	190	0	927	bottom
	190	190	0	835	top
	190	190	0	1218	top
II	200	200	250	325	top
	200	200	150	235	top
	200	200	150	381	top
	200	150	150	1020	bottom
	200	150	150	799	bottom
	200	150	150	937	top
	190	190	150	1140	top
	190	190	150	1272	top
	190	190	150	956	top

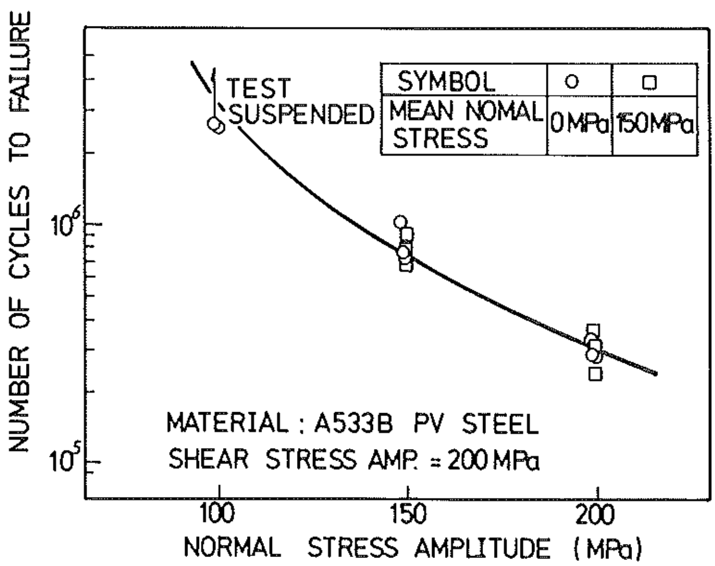

Fig 6 Effect of normal stress amplitude on fatigue life of A533B pressure vessel steel for a fixed value of maximum shear stress amplitude

of Group I show directly how normal stress amplitude reduces fatigue life for a fixed value of maximum shear stress amplitude. Comparison of sets Ib and Id, which had about the same lives, gives an indication of the relative influence of normal stress vs shear stress amplitude on life, but no quantitative influences can be drawn from such limited data.

Specimens from Group II show that mean normal stress had no significant influence in A533B for the test conditions used. There is an indication, from crack location, that tensile mean normal stress at top was slightly more detrimental than its compressive counterpart at bottom, as would be expected. Figure 6 shows clearly that normal stress amplitude has a significant influence on fatigue life for a fixed value of maximum shear stress amplitude.

Tests for mean bending stress effect

The lack of an observed mean normal stress influence with A533B steel, as shown in Table 6, is far from conclusive evidence. Any influence may have been diminished because the stress combinations used were high enough for some cyclic plastic straining to have occurred, permitting mean stress relaxation in these deflection controlled tests, in spite of efforts to avoid it. Consequently, further tests were performed to investigate the influence of mean bending stress on high-cycle, 90 degree out-of-phase bending and torsion fatigue, but with the higher strength SM45C steel.

Test program

Preliminary fatigue tests were conducted under alternating torsion and bending separately. The bending specimen and torsion specimen had the same geometry as given in reference (**15**). Tests were carried out to investigate the effect of mean bending stress on uniaxial bending fatigue of SM45C steel. A deflection-controlled, cantilever bending–torsion specimen, as shown in Fig. 5, was again used for the tests of mean bending stress effect on multiaxial fatigue. The 90 degree out-of-phase combinations of applied torsional and bending stresses with various K values were also selected to be low enough to minimize plastic straining.

Test results

Figure 7(a) illustrates the results of the preliminary fatigue tests. Mean bending stress clearly reduces the life in uniaxial bending fatigue. Failure was taken as a 10 per cent drop in specimen stiffness. Table 7 shows the test results of the mean bending stress effect on 90 degree out-of-phase bending and torsion fatigue. Equivalent stresses were calculated according to $SLEE$ with $\beta = 0.15$ (**15**) and $T/b = 0.7$ (from Fig. 7(a)) and these are plotted on Fig. 7(b). This figure shows that mean bending stress reduces the fatigue life.

Most cracks occurred where the mean stress was tensile, with directions along planes between 0 and 10 degrees to the transverse plane, and a few

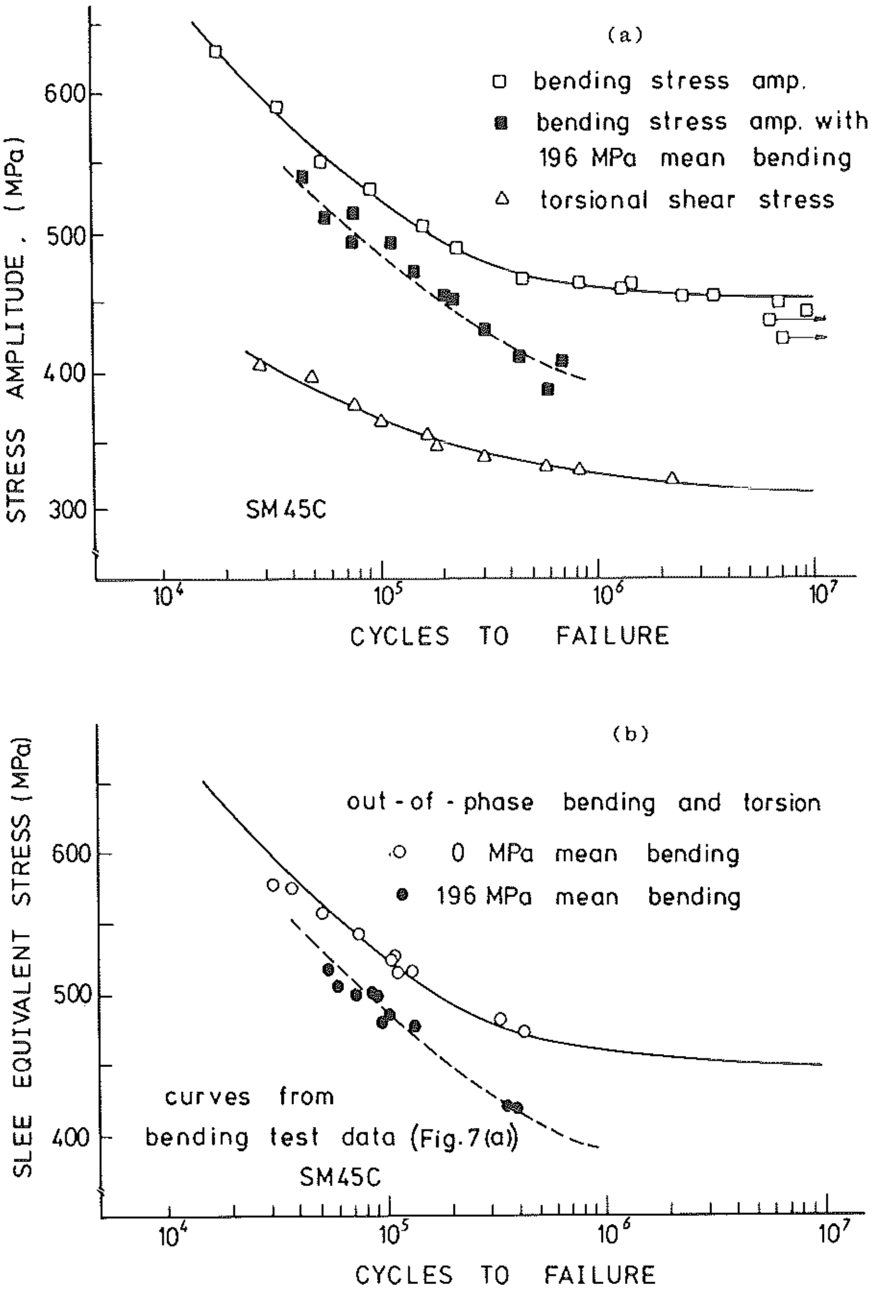

Fig 7 Stress versus fatigue life comparisons for SM45C steel: (a) stress amplitude data for fully reversed bending, repeated bending, and fully reversed torsion; (b) equivalent stress plots for 90 degree out-of-phase bending plus torsion with and without a mean bending stress

Table 7 Effect of mean bending stress on out-of-phase fatigue of SM45C structural steel

Group	Torsional stress amplitude (MPa)	Bending stress amplitude (MPa)	Bending mean stress (MPa)	Life (kilocycles)	Specimen
III	282	449	0	29.9	SM03
	334	354	0	35.7	SM08
	223	485	0	50	SM06
	309	357	0	73.8	SM02
	217	449	0	106	SM13
	285	370	0	106	SM01
	199	449	0	112	SM15
	194	457	0	131	SM04
	252	354	0	333	SM12
	154	437	0	431	SM14
	143	286	0	1660*	SM05
	165	354	0	1860*	SM07
IV	215	441	196	53	SM24
	309	286	196	59.2	SM23
	155	464	196	70.1	SM25
	136	473	196	86.3	SM16
	334	173	196	89.9	SM20
	209	403	196	92.1	SM21
	177	437	196	102	SM17
	321	167	196	135	SM19
	179	357	196	351	SM18
	274	182	196	394	SM22

* Tests suspended.

between 10 and 20 degrees for both Groups III and IV. Mean stress had no influence on crack direction in the intermediate to high-cycle multiaxial fatigue regime. A similar observation concerning crack direction in the presence of mean stress was reported in (**19**) for low-cycle multiaxial fatigue.

Discussion

A number of studies have now shown that the normal stress amplitude acting on planes of maximum amplitude of shear stress can have a secondary but significant influence on both proportional and non-proportional multiaxial fatigue. A similar trend was reported by Kanazawa *et al.* (**6**) on low cycle out-of-phase multiaxial fatigue. For potential use in design evaluations, a simplified, conservative relation between those two parameters, which can be applied to a variety of metals and different multiaxial straining conditions, is needed. Subject to further experimental verification, relations such as those suggested in (**20**)–(**22**) may prove useful in that regard, at least for constant amplitude loading and structural regions without notches. Relations proposed by Tipton and Nelson (**23**) may prove useful to assess multiaxial fatigue at notches. Considerable work lies ahead to develop life prediction methods to properly evaluate cumulative multiaxial fatigue damage.

The tests on SM45C steel have illustrated that mean bending stress can have an influence on non-proportional multiaxial fatigue if cyclic plastic straining does not eliminate the effects. In uniaxial fatigue, the modified Goodman line or the Gerber parabola are commonly used to predict the mean stress effect. These methods can be expressed as

$$S_f = S_a / \{1 - (S_m/S_u)^n\} \tag{9}$$

where S_a = alternating stress, S_m = mean stress, S_f = fully reversed stress which will provide the same life as the stress combination of alternating and mean stress, S_u = ultimate tensile strength, $n = 1$ for the modified Goodman line, and $n = 2$ for the Gerber parabola. In proportional or in-phase multiaxial fatigue, mean stress effects have been successfully correlated by Sines (**24**), and Kakuno and Kawada (**25**), but their criteria are not applicable for out-of-phase multiaxial fatigue loading.

In design evaluations of out-of-phase multiaxial fatigue with mean stress, a simplified, conservative relation between equivalent alternating stress and mean stress is necessary. For synchronous, out-of-phase bending and torsion with a mean bending stress ($\sigma = \sigma_m + \sigma_a \cos wt$, $\tau = \tau_a \cos(wt + \phi)$), the equivalent fully-reversed stress amplitude, $S_f\,(SLEE)$ can be obtained from equation (9) as follows

$$S_f\,(SLEE) = \sigma_a \left\{ 1 + \left(\frac{b}{2T} K \right)^{\alpha} \right\}^{1/\alpha} / \{1 - (S_m/S_u)^n\} \tag{10}$$

where $\alpha = 2(1 + \beta \sin \phi)$.

For the uniaxial bending fatigue data shown in Fig. 7(a), values of n were calculated with equation (9), being around 2 for lives less than 3×10^5 cycles, and around 1.5 for longer life. Figure 8(a) shows the life prediction using equation (9), with variable n taking $n = 2$ for lives shorter than 3×10^5 cycles and $n = 1.5$ otherwise, compared with the observed lives for uniaxial bending fatigue with a mean bending stress. Figure 8(b) shows the life prediction with constant $n = 2$.

Multiaxial fatigue lives for 90 degree out-of-phase bending and torsion with mean bending stress are predicted with equation (10) using the same variable n values as in Fig. 8(a) and compared with the observed lives. Figure 9(a) shows that fatigue life of the SM45C steel is closely correlated by $S_f\,(SLEE)$ with observed life. To compare the accuracy of mean stress predictions from the maximum shear stress criterion ($SALT$), and the octahedral shear stress criterion ($SEQA$), the parameter S_a in equation (9) is replaced by $SALT$ and $SEQA$ to obtain $S_f\,(SALT)$ and $S_f\,(SEQA)$, respectively. Predictions by S_f ($SALT$) and $S_f\,(SEQA)$ are shown in Fig. 9(b) and (c), which clearly show that $SALT$ and $SEQA$, modified for mean stress effects, are not adequate theories.

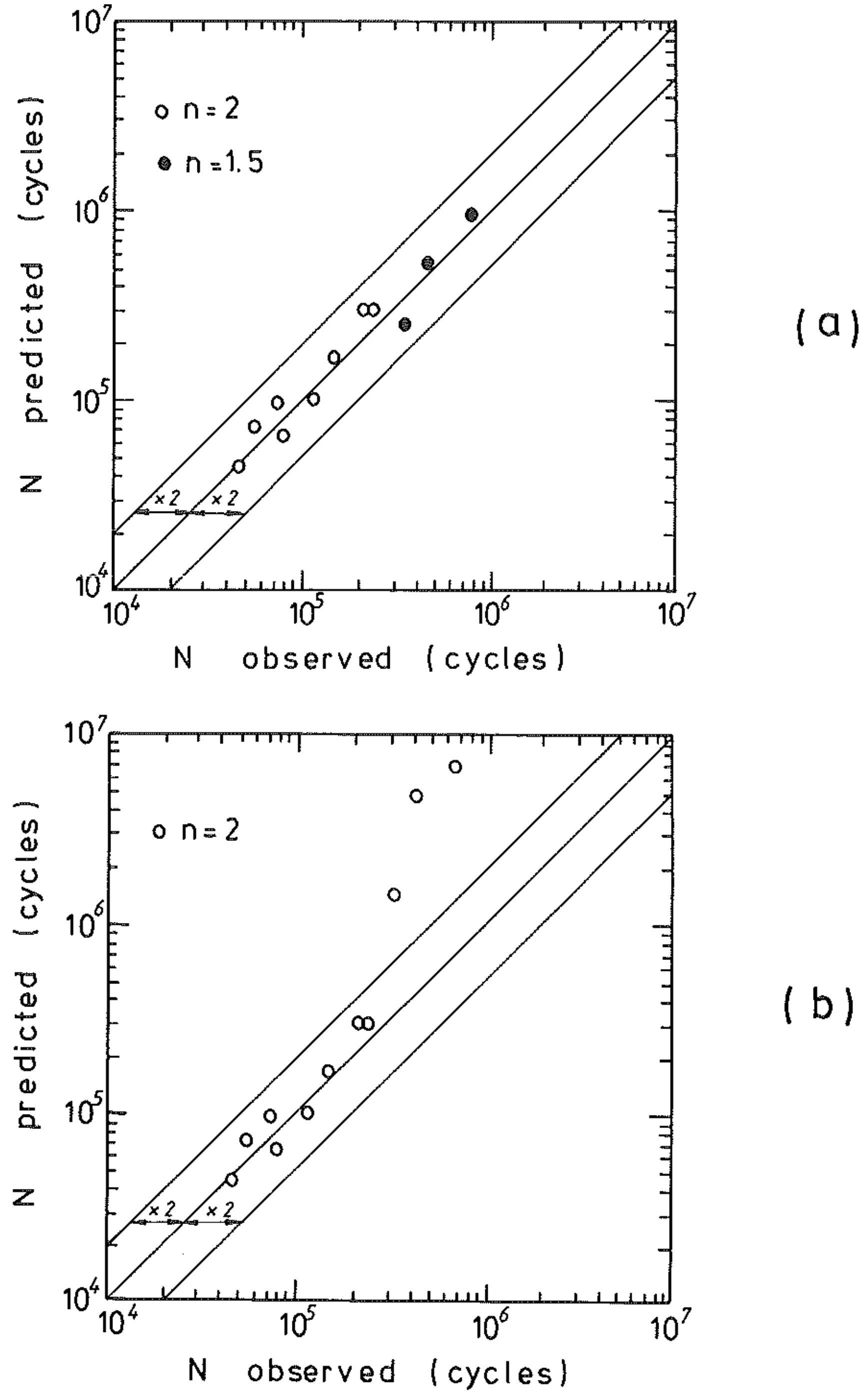

Fig 8 Comparison of life predictions based on equation (10) with uniaxial bending fatigue data of SM45C steel, (a) with variable n taking $n = 2$ for lives under 3×10^5 cycles and $n = 1.5$ otherwise, (b) with constant $n = 2$

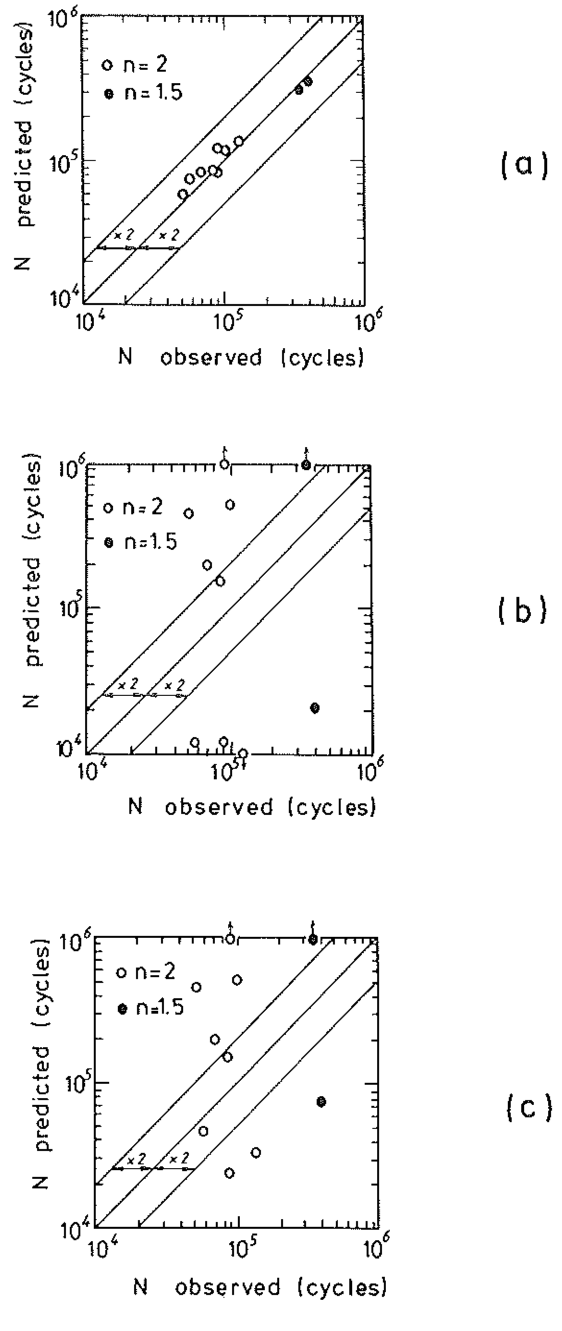

Fig 9 Comparisons of life predictions with multiaxial fatigue data of SM45C steel under 90 degree out-of-phase bending and torsion: (a) predictions by S_f (*SLEE*); (b) predictions by S_f (*SALT*); (c) predictions by S_f (*SEQA*)

Conclusions

(1) Test results using discriminating specimens have provided additional evidence that the recent criterion due to Lee is an adequate predictor for out-of-phase bending and torsion, for type 304 stainless and A533B pressure vessel steels.
(2) The magnitude of normal stress amplitude on a plane of maximum shear stress amplitude had a significant influence on fatigue life in 90 degree out-of-phase bending-torsion tests on A533B steel.
(3) Mean bending stress reduced fatigue life in 90 degree out-of-phase bending-torsion tests of SM45C steel. The influence of mean bending stress on out-of-phase bending and torsion fatigue life, predicted by combining the Lee criterion with a uniaxial mean stress effect criterion, was in good agreement with test results of the higher strength SM45C steel.

Acknowledgements

The research for this paper was performed with support from the Electric Power Research Institute and the National Science Foundation through the Stanford Center for Materials Research, and the Korea Ministry of Science and Technology.

Professor H. O. Fuchs provided invaluable guidance on, and encouragement in, the use of the discriminating specimen approach. Professor D. V. Nelson made a significant contribution on the tests for normal stress influence. Tests with SM45C steel were carried out by Mr Hak-Joo Lee.

References

(1) BROWN, M. W. and MILLER, K. J. (1973) A theory for fatigue failure under multiaxial stress–strain conditions, *Proc. Instn mech. Engrs*, **187**, 754–755.
(2) KREMPL, E. (1974) The influence of state of stress on low cycle fatigue of structural materials, *ASTM STP 549*, American Society for Testing and Materials, Philadelphia, PA.
(3) GARUD, Y. S. (1981) Multiaxial fatigue: a survey of the state of the art, *J. Testing Eval.*, **9**, 165–178.
(4) LITTLE, R. E. (1969) A note on the shear criterion for fatigue under combined stress, *Aeronaut. Q.*, **20**, 57–60.
(5) DIETMANN, H. and LEMPP, W. (1979) Untersuchungen zum Festigkeitsverhalten von Stahlen bei mehrachsiger phasenverschobener Dauerschwingbeanspruchchung, *Konstrucktion*, **31**, 191–200.
(6) KANAZAWA, K., MILLER, K. J., and BROWN, M. W. (1977) Low-cycle fatigue under out-of-phase loading conditions, *J. Engng Mater. Technol.*, **99**, 222–228
(7) HULL, W. C. (1977) A rational theory of failure for combined stress high-cycle fatigue, *Proc. of the ASME Design Engineering Technology Conference*, American Society of Mechanical Engineers, New York, pp. 179–195.
(8) GRUBISIC, V. and SIMBÜRGER, A. (1976) Fatigue under combined out-of-phase multiaxial stresses, *Proc. of the International Conf. on Fatigue Testing and Design*, Society of Environmental Engineers, London, pp. 27.1–27.8.
(9) McDIARMID, D. L. (1977) A criterion of fatigue failure under out-of-phase multiaxial stresses, *Proc. of the Sixth Canadian Conf. on Applied Mechanics*, Vancouver, pp. 245–246.

(10) FINDLEY, W. N. (1959) A theory for the effect of mean stress on fatigue of metals under combined torsion and axial load or bending, *J. Engng Ind.*, **81**, 301–306.

(11) FUCHS, H. O. (1979) Fatigue research with discriminating specimens, *Fatigue Engng Mater. Structures*, **2**, 207–215.

(12) LANGER, B. F. (1979) Design of pressure vessels involving fatigue, *Pressure Vessel Engineering* (Edited by NICHOLS, R. W.), Elsevier, Amsterdam, pp. 59–100.

(13) *ASME Boiler and Pressure Vessel Code* (1974) Section III, Div. 1, Subsection NA, Appendix XIV, American Society of Mechanical Engineers, New York.

(14) LEE, S. B. (1980) *Evaluation of theories on multiaxial fatigue with discriminating specimens*, PhD thesis, Stanford University.

(15) LEE, S. B. (1985) A criterion for fully reversed out-of-phase torsion and bending, *Multiaxial Fatigue, ASTM STP 853*, American Society for Testing and Materials, Philadelphia, PA, pp. 553–568.

(16) *Cases of the ASME Boiler and Pressure Vessel Code* (1978) Code Case N–47–12, American Society of Mechanical Engineers, New York.

(17) GOUGH, H. J. (1950) Engineering steels under combined cyclic and static stresses, *J. Appl. Mech.*, **72**, 113–125.

(18) GOUGH, H. J., POLLARD, H. V., and CLENSHAW, W. J. (1951) *Some experiments on the resistance of metals to fatigue under combined stress*, Memo 2522, Aeronautical Research Council, HMSO, London.

(19) SOCIE, D. F., WAILL, L. A., and DITTMER, D. F. (1985) Biaxial fatigue of Inconel 718 including mean stress effects, *Multiaxial Fatigue, ASTM STP 853*, American Society for Testing and Materials, Philadelphia, PA, pp. 463–481.

(20) LOHR, R. D.. and ELLISON, E. G. (1980) A simple theory for low cycle multiaxial fatigue, *Fatigue Engng Mater. Structures*, **3**, 1–17.

(21) McDIARMID, D. L. (1974) A new analysis of fatigue under combined bending and twisting, *Aeronaut. J.*, **78**, 325–359.

(22) BLASS, J. J. (1977) Assessment of multiaxial fatigue criteria, *High Temperature Structural Design Program Progress Report*, ORNL-5374, Oak Ridge National Laboratory, pp. 117–126.

(23) TIPTON, S. M. and NELSON, D. V. (1985) Fatigue life predictions for a notched shaft in combined bending and torsion, *Multiaxial Fatigue, ASTM STP 853*, American Society for Testing and Materials, Philadelphia, PA, pp. 514–550.

(24) SINES, G. (1955) Failure of materials under combined repeated stresses with superimposed static stresses, *NACA TN 3495*.

(25) KAKUNO, H. and KAWADA, Y. (1979) A new criterion of fatigue strength of a round bar subjected to combined static and repeated bending and torsion, *Fatigue Engng Mater. Structures*, **2**, 229–236.